

Magnetic versus nonmagnetic doping effects on the magnetic ordering in the Haldane chain compound $\text{PbNi}_2\text{V}_2\text{O}_8$

Andrej Zorko and Denis Arčon

Jozef Štefan Institute, Jamova 39, 1000 Ljubljana, Slovenia

Alexandros Lappas

Institute of Electronic Structure and Laser, Foundation for Research and Technology – Hellas, P.O. Box 1527, 71110 Heraklion, Crete, Greece

Zvonko Jagličić

Institute of Mathematics, Physics and Mechanics, Jadranska 19, 1000 Ljubljana, Slovenia

(Dated: March 23, 2024)

A study of an impurity driven phase-transition into a magnetically ordered state in the spin-liquid Haldane chain compound $\text{PbNi}_2\text{V}_2\text{O}_8$ is presented. Both, macroscopic magnetization as well as ^{51}V nuclear magnetic resonance (NMR) measurements reveal that the spin nature of dopants has a crucial role in determining the stability of the induced long-range magnetic order. In the case of nonmagnetic (Mg^{2+}) doping on Ni^{2+} spin sites ($S = 1$) a metamagnetic transition is observed in relatively low magnetic fields. On the other hand, the magnetic order in magnetically (Co^{2+}) doped compounds survives at much higher magnetic fields and temperatures, which is attributed to a significant anisotropic impurity-host magnetic interaction. The NMR measurements confirm the predicted staggered nature of impurity-liberated spin degrees of freedom, which are responsible for the magnetic ordering. In addition, differences in the broadening of the NMR spectra and the increase of nuclear spin-lattice relaxation in doped samples, indicate a diverse nature of electron spin correlations in magnetically and nonmagnetically doped samples, which begin developing at rather high temperatures with respect to the antiferromagnetic phase transition.

PACS numbers: 75.30.Kz, 75.40.-s, 76.60.-k

I. INTRODUCTION

Highly correlated quantum spin systems exhibit a variety of intriguing magnetic phenomena in reduced dimensions. Impurities introduced to such systems have been in the past successfully employed to reveal the magnetic character of host materials. The virtue of magnetic doping and boundaries created by nonmagnetic dopants is to introduce novel degrees of freedom. Study of electronic structure and electron spin correlations in the vicinity of the impurity sites is essential for understanding the quantum state of the host. This approach has been, for instance, widely exploited in the quest of finding an interconnection between magnetic and superconducting nature of high- T_c cuprates.^{1,2} Similarly, doping turned out to be an irreplaceable source of information about the ground state in various other transition-metal oxides exhibiting macroscopically coherent ground states, such as singlet ground states in $S = 1=2$ spin-Peierls chains,³ spin ladders⁴ and Haldane integer-spin chains,⁵ which all show a spin gap in their excitation spectrum.

Common consequences of the nonmagnetic impurities embedded in low-dimensional antiferromagnets include an enhancement of antiferromagnetic correlations and an induction of staggered magnetic moments near the impurity sites. These effects are manifested in the vicinity of vacancies in one-dimensional⁶ and two-dimensional⁷ antiferromagnetic Heisenberg lattices with gapless excitations, as well as in spin-gap systems with robust nonmag-

netic ground states including spin-Peierls chains,^{8,9} spin ladders¹⁰ and Haldane chains.^{11,12} For this reason, it was argued that the enhanced correlations at short distances have a common origin independent of the long-distance behavior of the spin correlations. The enhancement can be explained within the so-called “pruned” resonating-valence-bond picture to be a consequence of pruning the possible singlet configurations for spins close to the vacancy sites.^{8,9} The staggered magnetic moments have been recently observed also experimentally in the case of nonmagnetic^{13,14} and magnetic¹⁴ doping of the Haldane chain compound Y_2BaNiO_5 , where exponentially decaying staggered magnetization was detected next to the impurities, with the staggered moments only weakly dependent on the magnetic nature of the dopants.

A rather unexpected feature observed in different one-dimensional spin-gap systems is the presence of long-range magnetic ordering induced by impurities.^{3,4,15,16} The ordering is believed to originate from the impurity-induced staggered moments. These moments are coupled along the chains with an exponentially decaying staggered exchange,¹² because the coupling is mediated by virtual excitations of the gaped medium.¹⁷ Obviously, interchain coupling is vital for providing foundations for the three-dimensional magnetic ordering.¹⁸ There have been few attempts, recently published, trying to unify the field of the impurity-induced magnetic ordering. For instance, Mélin et al.¹⁷ highlighted the role of three characteristic temperatures in doped spin-gap systems; namely, the

temperature below which spin correlations within chains begin to develop, the typical energy of the staggered exchange, and the Stoner temperature of the order of the interchain coupling, associated with the development of three-dimensional magnetic correlations. The relative amplitudes of the latter two have been argued to determine whether the impurity-induced long-range ordering should be present. Although there is a great deal of reports on long-range ordering as a consequence of doping different spin-gap systems, a comprehensive theory capable of “predicting” the observed transition temperatures and the stability of the induced long-range magnetically ordered states upon external perturbations such as magnetic field, still does not seem to be within reach. Moreover, the effect of the magnetic character of the dopants on magnetic ordering is particularly vague and, therefore, implores for further investigation.

The purpose of this paper is, therefore, to provide a further experimental insight into the complex problem of the impurity-induced phenomena regarding the magnetism of spin-gap systems. The emphasis is put on the comparison between magnetic and nonmagnetic doping of the Haldane-chain compound $\text{PbNi}_2\text{V}_2\text{O}_8$, possessing chains of Ni^{2+} spins ($S = 1$), with a by far dominant nearest-neighbor (nn) intrachain exchange coupling $J = 95$ K (in units of k_B).¹⁶ dc magnetization measurements are used to explore the temperature as well as the magnetic-field stability of the impurity-induced long-range magnetic order. In addition, nuclear magnetic resonance (NMR) measurements on ^{51}V nuclei weakly coupled to the system of localized electronic moments through a transferred hyperfine coupling, are exploited as a local-probe technique, capable of detecting the inhomogeneities as well as the dynamics in the electron spin system. We show that the magnetic nature of the dopants plays a crucial role in reducing quantum fluctuations in Haldane chains and thus helps stabilizing the magnetic long-range order. Moreover, it dictates the character of the electron spin correlations at low-temperatures.

II. EXPERIMENTAL

All the samples used in this investigation were prepared according to the same solid-state reaction procedure.¹⁹ The resulting polycrystalline powders can be addressed as solid solutions, since the Mg^{2+} and Co^{2+} substitutions for Ni^{2+} ions are randomly distributed. Phase purity of the samples was verified by powder x-ray and neutron diffractometry,^{19,20,21} which revealed that the effect of the impurities on the position of all the ions within the unit cell is minor. The same samples were used in our previous report presenting combined results of electron spin resonance (ESR) and magnetization measurements in low magnetic field.²²

Bulk magnetic measurements were performed with a Quantum Design SQUID magnetometer. dc magnetization was obtained from field-cooled runs between room

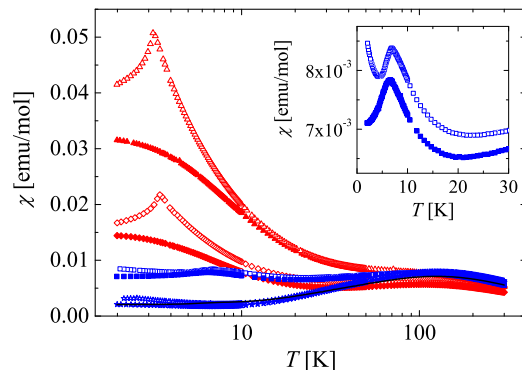


FIG. 1: (Color online) dc susceptibility in $\text{PbNi}_2\text{V}_2\text{O}_8$ (solid line), nonmagnetically doped $\text{PbNi}_{1.88}\text{Mg}_{0.12}\text{V}_2\text{O}_8$ (diamonds) and $\text{PbNi}_{1.76}\text{Mg}_{0.24}\text{V}_2\text{O}_8$ (triangles), as well as magnetically doped $\text{PbNi}_{1.98}\text{Co}_{0.02}\text{V}_2\text{O}_8$ (stars) and $\text{PbNi}_{1.92}\text{Co}_{0.08}\text{V}_2\text{O}_8$ (squares) in magnetic fields of 0.1 T (open symbols) and 5 T (full symbols and solid line). The inset shows a decrease of the low-temperature peak position with increased field in the $\text{PbNi}_{1.92}\text{Co}_{0.08}\text{V}_2\text{O}_8$ compound.

temperature and 2 K in static magnetic fields of 0.1 T and 5 T.

^{51}V NMR measurements were conducted by standard pulsed NMR techniques in an external magnetic field of 6.34 T in the temperature range between room temperature and 4.2 K. Typical width of applied $\pi/2$ pulses was 6 μs . Due to the rather broad NMR spectra the spectral width of such pulses was insufficient to reliably detect the full spectra even at room temperature. For this reason, the NMR spectra were obtained in frequency-sweep experiments from the amplitude of the Hahn-echo-detected signals. ^{51}V spin-lattice relaxation was investigated by employing a saturation-recovery method.

III. RESULTS

A. dc magnetization

Upon doping, the $\text{PbNi}_2\text{V}_2\text{O}_8$ compound undergoes a phase transition from the spin-liquid Haldane state into the long-range magnetically ordered state.¹⁶ The antiferromagnetic nature of the observed ordering was confirmed by additional Bragg peaks in neutron diffraction patterns observed below the phase-transition temperature.¹⁹ The ordering can also be detected by dc magnetization measurements, which show clear peaks in dc susceptibility at the phase-transition temperature. In Fig. 1 such measurements are presented for two Mg-doped compounds, $\text{PbNi}_{1.88}\text{Mg}_{0.12}\text{V}_2\text{O}_8$ and $\text{PbNi}_{1.76}\text{Mg}_{0.24}\text{V}_2\text{O}_8$, and two Co-doped samples, $\text{PbNi}_{1.98}\text{Co}_{0.02}\text{V}_2\text{O}_8$ and $\text{PbNi}_{1.92}\text{Co}_{0.08}\text{V}_2\text{O}_8$. In accordance with the previous measurements,^{21,23} the phase transition in an external magnetic field of

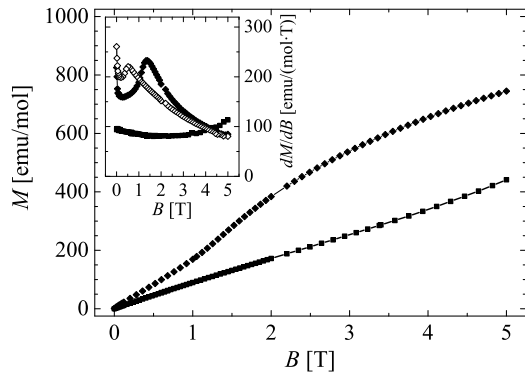


FIG. 2: Magnetization curves for $\text{PbNi}_{1.88}\text{Mg}_{0.12}\text{V}_2\text{O}_8$ (diamonds) and $\text{PbNi}_{1.92}\text{Co}_{0.08}\text{V}_2\text{O}_8$ (squares) measured at 2 K. Inset shows the derivative of both curves as well as of the curve measured in the former compound at 3.2 K (open diamonds).

0.1 T is observed in nonmagnetically doped samples $\text{PbNi}_{1.88}\text{Mg}_{0.12}\text{V}_2\text{O}_8$ and $\text{PbNi}_{1.76}\text{Mg}_{0.24}\text{V}_2\text{O}_8$ at 3.4 K and 3.2 K, respectively, while it is shifted to 7.1 K in the magnetically doped $\text{PbNi}_{1.92}\text{Co}_{0.08}\text{V}_2\text{O}_8$ compound. The transition in the lightly doped $\text{PbNi}_{1.98}\text{Co}_{0.02}\text{V}_2\text{O}_8$ compound is found around 2.6 K, similarly as reported elsewhere.²⁴

The magnitude of the impurity-induced low-temperature dc susceptibility substantially depends on the spin nature of the dopants as shown in Fig. 1. This was successfully attributed to the magnetic coupling between the impurity and the impurity-liberated spins in our previous report.²² Based on the impurity-host antiferromagnetic coupling in Co-doped samples, $J_{\text{ih}} = 14$ K, and the effective ferromagnetic coupling between spins neighboring a particular impurity site, $J^0 = 2$ K, both derived from the ESR investigations, we were able to give a quantitative description of the observed phenomenon.

Upon increasing the static magnetic field up to 5 T, the peak in the dc susceptibility disappears in the case of Mg-doping. On the other hand, the peak is only slightly displaced to 6.5 K in the $\text{PbNi}_{1.92}\text{Co}_{0.08}\text{V}_2\text{O}_8$ compound as shown in the inset of Fig. 1. The latter observation together with the significantly increased phase-transition temperature in this sample indicate enhanced stability of the magnetic order in the cobalt doped samples. The disappearance of the phase transition in relatively low magnetic fields of the order of few Tesla has already been reported for lightly Mg-doped compounds²⁵ as well as for the heavily doped $\text{PbNi}_{1.76}\text{Mg}_{0.24}\text{V}_2\text{O}_8$ compound.¹⁹ In the latter case, a field-induced metamagnetic transition was suggested based on the dc and ac susceptibility results. Similar behavior is found also in the $\text{PbNi}_{1.88}\text{Mg}_{0.12}\text{V}_2\text{O}_8$ sample. More specifically, within the magnetically ordered phase the field dependence of the magnetization curve exhibits a pronounced inflection

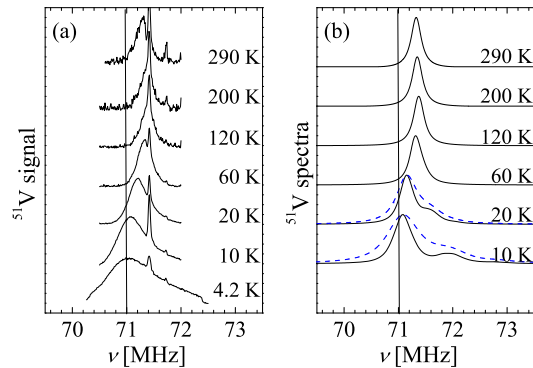


FIG. 3: The collection of (a) measured and (b) simulated ^{51}V NMR spectra in $\text{PbNi}_{1.88}\text{Mg}_{0.12}\text{V}_2\text{O}_8$. Fits represented by solid lines are based on the assumption of temperature independent homogeneous broadening, while dashed lines correspond to temperature dependent broadening.

point (see Fig. 2), typical of the second order phase transition from the antiferromagnetically ordered to the paramagnetic phase.²⁶ Such transition can be recognized to occur around 1.4 T at 2 K, corresponding to the peak in the derivative of the magnetization curve. The critical field decreases with temperature. For instance, the peak is observed around 0.5 T at 3.2 K (see Fig. 2).

On the contrary, in $\text{PbNi}_{1.92}\text{Co}_{0.08}\text{V}_2\text{O}_8$ a linear dependence of the magnetization curve is detected up to 4 T at 2 K (see Fig. 2). The curvature of the magnetization curve is slightly enhanced above 4 T as expressed in its derivative, however, it seems that even a magnetic field of 5 T is still appreciably below the critical field value, which would destroy the magnetic order. The antiferromagnetic order in Co-doped samples obviously persists to much higher magnetic fields, which is also in line with the results of the NMR measurements presented below.

B. NMR measurements

We have already reported on ^{51}V ($I = 7/2$) NMR measurements in the pristine $\text{PbNi}_2\text{V}_2\text{O}_8$ compound as well as in its Mg-substituted derivatives.²⁷ The temperature evolution of the NMR spectra for the latter case is shown in Fig. 3(a) and Fig. 4(a). We focus our attention on the broad spectra. A sharp resonance at 71.72 MHz is due to the presence of ^{63}Cu nuclei at or around our probe. Similarly, the additional narrow component at around 71.42 MHz, observed in both Mg-doped samples will also be neglected in the following analysis, as it shows no indications of coupling of the detected nuclei to the electron spin system.²⁷

At room temperature the NMR absorption spectra of both Mg-doped samples look qualitatively the same as those of the pristine compound.²⁷ They can be explained by the Hamiltonian

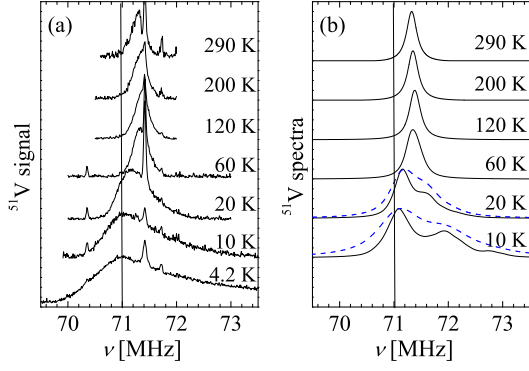


FIG. 4: The ^{51}V NMR spectra (a) measured and (b) simulated for the case of $\text{PbNi}_{1.76}\text{Mg}_{0.24}\text{V}_2\text{O}_8$. As in the previous figure, solid and dashed lines correspond to simulations based on temperature independent and temperature dependent homogeneous broadening, respectively.

$$H = H_Z + H_Q + H_{hf} + H_{cs}; \quad (1)$$

where the first term corresponds to the Zeeman energy of ^{51}V nuclear spins \mathbf{I}_i in the external magnetic field \mathbf{B}_0 , the second term H_Q represents the quadrupolar coupling of nuclear quadrupolar moments with electric field gradients, the hyperfine term H_{hf} originates from the transferred hyperfine coupling of vanadium nuclear spins with surrounding nickel electron spins \mathbf{S}_j , and H_{cs} corresponds to the chemical-shift Hamiltonian. The broad structure of the spectra observed at room temperature originates from the quadrupolar coupling with the consecutive satellite transitions displaced by $\nu_Q \approx 80$ kHz.²⁸ On the other hand, a pronounced broadening of the central transition ($1=2 \rightarrow 1=2$) is due to the anisotropy of the chemical shift tensor.²⁸ Further, the isotropic part of the transferred hyperfine interaction plays the dominant role in determining the NMR shift. This fact is most clearly manifested in a gap-like behavior of this parameter, which thus scales with the bulk uniform susceptibility of the parent compound.²⁸

To evaluate the ^{51}V NMR frequency shift the standard VOCl_3 compound was utilized. Its ^{51}V NMR spectrum is positioned at $\nu_L^{\text{dia}} = 70.974$ MHz in our magnetic field. Since the measured frequency shift in the $\text{PbNi}_2\text{V}_2\text{O}_8$ sample is a combined contribution of the isotropic part of the transferred hyperfine interaction and the isotropic part of the chemical shift tensor, the Larmor frequency of exactly $\nu_L^0 = 71.0$ MHz corresponding to the pristine compound at 4.2 K, can be used for setting the reference of a zero paramagnetic shift. Namely, at such low temperatures the spin susceptibility on the Haldane spin system should be diminished due to its activated behavior. The value ν_L^0 is presented in our figures with NMR spectra by horizontal lines.

When lowering the temperature, the spectra of the Mg-doped compounds exhibits a pronounced broadening with respect to the parent compound, which shows

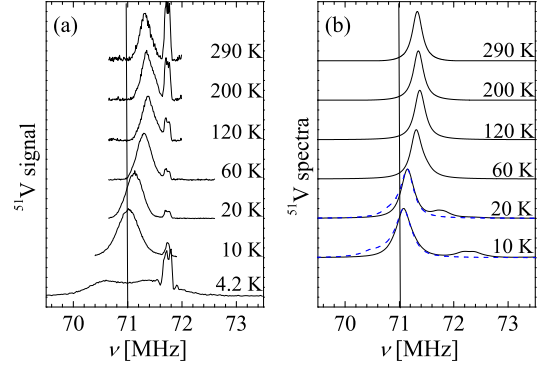


FIG. 5: The temperature evolution of (a) measured and (b) simulated ^{51}V NMR spectra in $\text{PbNi}_{1.92}\text{Co}_{0.08}\text{V}_2\text{O}_8$. The fits correspond to paramagnetic order (solid lines) and antiferromagnetic (dashed lines) correlations between impurity and impurity-induced spins.

practically unchanged linewidth in the whole investigated temperature range. We have previously speculated that this experimental finding should be a precursor effect of the three-dimensional magnetic ordering in both Mg-doped compounds.²⁷ In this paper, we offer a quantitative description of the broadening effect, which is based on the temperature evolution of the size of the impurity-induced staggered moments as well as on the development of the three-dimensional correlations between them.

Contrary to the case of the nonmagnetic Mg^{2+} doping, magnetic Co^{2+} dopants have a completely different impact on the evolution of the ^{51}V NMR spectra. As shown in Fig 5(a), in $\text{PbNi}_{1.92}\text{Co}_{0.08}\text{V}_2\text{O}_8$ the spectra show less pronounced broadening with decreasing temperature. They, however, exhibit a drastic change in their width and appearance (two-peak structure) below 6 K, signaling the transition into the magnetically ordered state. The broadening effect is even more reduced in the case of the $\text{PbNi}_{1.98}\text{Co}_{0.02}\text{V}_2\text{O}_8$ compound as presented in the next section. The observation of broader NMR spectra in nonmagnetically doped compounds than in magnetically doped samples seems surprising since magnetic impurities are expected to be coupled to the vanadium nuclei in contrast to the vacant magnesium sites. Thus, at least close to the phase-transition temperature Co^{2+} impurities should significantly contribute to the appearance of the NMR spectra due to slowing-down of the electron spin fluctuations.

To get a further insight into the temperature development of the electron spin correlations, we also performed ^{51}V NMR spin-lattice relaxation measurements. Due to strong transferred hyperfine coupling the spin-lattice relaxation is expected to be mainly caused by transverse electron spin fluctuations.^{29,30} When the temperature is lowered a rather diverse behavior is observed in different samples. The monotonic decrease of the parameter $(T_1 T)^{-1}$ with decreasing temperature as observed in the

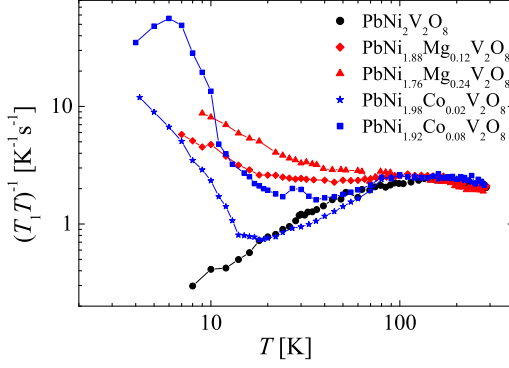


FIG. 6: (Color online) The temperature dependence of the ^{51}V NMR spin-lattice relaxation rate (divided by temperature) in the parent and the impurity doped $\text{PbNi}_2\text{V}_2\text{O}_8$ compounds.

parent compound, is characteristic of the Haldane-gap excitations.³¹ On the other hand, the low-temperature up-turn in all doped samples gives a clear indication of the developing electron spin correlations, as discussed further in the next section. A rather surprising observation is again the fact that the low-temperature deviations of the $(T_1T)^{-1}$ in Mg-doped samples with respect to the pristine compound are observed from much higher temperatures than in Co-doped samples, while at the same time the increase of this parameter is much more moderate in the case of the nonmagnetic impurities. Similarly to the bulk magnetic measurement and the temperature evolution of the NMR spectra, these experimental findings again indicate on the impurity dependent character of the electron spin correlations.

IV. ANALYSIS AND DISCUSSION

A. Frequency shift and broadening of the ^{51}V NMR spectra in doped compounds

As already mentioned in the preceding section, the room-temperature lineshape of the ^{51}V NMR spectra in the parent as well as in all the doped samples is determined by the quadrupolar Hamiltonian and the anisotropic part of the chemical shift tensor. In addition, the relatively large shift of the spectra, i.e., $\delta = \frac{\delta}{\nu_L} = 0.4\%$, can be attributed to the transferred hyperfine coupling between the vanadium nuclei and the electron magnetic moments localized on Ni^{2+} (and impurity) sites,

$$H_{\text{hf}} = \sum_{i,j} \mathbf{I}_i \cdot \mathbf{A}_j \cdot \mathbf{S}_j \quad (2)$$

where the sums run over all the vanadium nuclei (\mathbf{I}_i) and over its six nearest-neighbor Ni^{2+} sites (\mathbf{S}_j).^{20,28} Although isolated V^{5+} ions are diamagnetic, they can

be addressed as being partially magnetic³² in the $\text{PbNi}_2\text{V}_2\text{O}_8$ compound. This is due to the imbalance in the closed vanadium electronic shells caused by the interaction of vanadium and nickel electrons, which results in the effective transferred hyperfine coupling between the ^{51}V nuclear spins and the Ni^{2+} electron spins. In powder samples only the isotropic part of the hyperfine tensor contributes to the shift of the NMR spectra, which allows us to estimate this coupling as

$$A_{ij}^{\text{iso}} = \frac{2h}{6} \frac{N_A g_B}{m_{\text{ol}} B_0} = 0.17 \text{ mK} : \quad (3)$$

In the above estimation we used the room-temperature value of the molar susceptibility in the magnetic field of 5 T, $m_{\text{ol}} = 5.6 \cdot 10^{-3} \text{ emu/mol}$, as a measure of the average value of the nickel spins in the parent material $\hbar S_j^0 = m_{\text{ol}} B_0 = 2 N_A g_B$. Room-temperature g -factor value $g = 2.2$ was determined by ESR measurement.³³

In doped Haldane chains impurity-induced staggered magnetic spins $\hbar S_j^{\pm 1}$ are expected to be superimposed on the uniform spin chain, defining the average spin value at each site as

$$\hbar S_j = S_j^0 + S_j^{\pm 1} : \quad (4)$$

An NMR detection of the staggered magnetization near impurity sites has been, in fact, recently reported in another Haldane chain compound Y_2BaNiO_5 .¹³ The authors observed additional peaks shifted to lower and higher frequencies with respect to the main NMR line of the ^{89}Y nuclei being coupled to single Ni^{2+} sites. These lines were attributed to the yttrium nuclei coupled to the staggered moments, with exponentially decaying correlations. The temperature dependence of the correlation length was shown to follow nicely theoretical predictions,³⁴ while the amplitude of the staggered moments exhibited Curie-dependence for $S = 1/2$ spins, in the case of nonmagnetic Zn^{2+} as well as magnetic Cu^{2+} dopants.¹⁴ Well defined chain-end excitations, experimentally observed also at temperatures far above the Haldane gap, were theoretically reproduced by quantum Monte Carlo calculations,³⁵ which justified the simple decomposition of the average spin value given by Eq. (4) in a broad temperature range.

The shift of the NMR spectra in doped $\text{PbNi}_2\text{V}_2\text{O}_8$ compounds should reflect the impurity-induced contribution to the dc magnetization of these compounds. In Fig. 7(a) the temperature dependence of the first moment of the measured ^{51}V NMR spectra is presented. In the case of the nonmagnetic Mg-doping the expected up-turn in the NMR shift is observed at low temperatures, however, the increase of the low-temperature dc susceptibility is much more pronounced (see Fig. 1). Disagreement between the two quantities is even more obvious in the case of the magnetic Co-doping. Here, the impurity contribution to the magnetization observed in the dc susceptibility at low-temperatures is not reflected in the shift of the NMR spectra at all. Although, at first sight, these

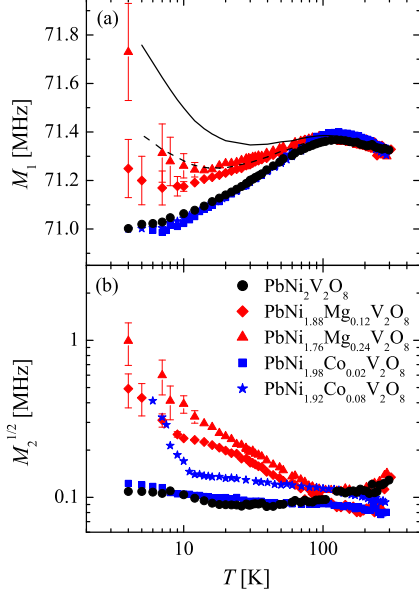


FIG. 7: (Color online) The temperature dependence of the ^{51}V NMR (a) line position and (b) linewidth in doped $\text{PbNi}_2\text{V}_2\text{O}_8$ compounds. The lines correspond to the model explained in the Section IV B.

observations would suggest that our NMR measurements can not detect the impurity-induced staggered magnetization, we prove in the subsequent subsection that this is not the case. Namely, the fact that vacant sites (Mg^{2+} impurities) produce shifts towards lower frequencies and that Co^{2+} impurities induce weaker hyperfine coupling to ^{51}V nuclei, prove to be essential.

The linewidth (second moment) of the NMR spectra also significantly depends on the spin nature of the dopants [Fig. 7(b)]. The broadening with lowering temperature for the Mg-doped samples is tremendous and starts at rather high temperatures with respect to the phase-transition temperature in low magnetic fields. On the other hand, the Co-doped samples show much more moderate broadening in the paramagnetic phase and a significant increase of the linewidth in the vicinity of the phase transition, characteristic of critical effects, as explained below. This fact implies on a diverse nature of the spin correlations determining the low-temperature NMR lineshape in both cases, which is in line with the drastically different stability of the magnetically ordered phase.

B. Simulation of the ^{51}V NMR spectra

Contrary to the ^{89}Y ($I = 1/2$) case in Y_2BaNiO_5 ,^{13,14} the NMR spectra of the ^{51}V nuclei in $\text{PbNi}_2\text{V}_2\text{O}_8$ are quadrupolarly broadened. For this reason, the impurity-induced inhomogeneities of the spin density sensed by

vanadium nuclei are hidden within the spectra at high temperatures. For instance, at room temperature a spin following the Curie dependence and corresponding to the $S = 1/2$ degree of freedom induces according to Eq. (3) a frequency shift of $\nu_i = 30$ kHz at the ^{51}V nucleus, to which it is coupled. This value should be compared to the width of the room-temperature experimental spectra, approximately given by $2\nu_0 = 160$ kHz. However, at lower temperatures the impurity-generated features of the NMR spectra are expected to come into sight.

Trying to construct a quantitative picture of the above-mentioned effects, we performed the following simulation procedure. In a finite spin chain ($N = 4096$) the impurity positions with a given concentration were randomly distributed. The uniform part $\langle S_j^z \rangle$ of the average spin value at a certain temperature was deduced from the temperature dependence of the position of the ^{51}V NMR spectra in the pristine compound. The contribution of the staggered moments, $\langle S_j^z \rangle$, was calculated from the position of all impurities, taking into account the staggered nature of the impurity-induced moments with the theoretically predicted temperature-dependent correlation length³⁴ and assuming the magnitude of these moments to be given by the Brillouin function, $S = B(g_B S_B / k_B T)$. In addition, in the case of Co-doping, the spin of the impurities $S_i = 3/2$, following the Curie dependence, was also taken into consideration. The average spin value interacting with a particular ^{51}V nucleus was then calculated as a sum of four consecutive spins on Ni^{2+} sites in one chain and two spins in its neighboring chain. Namely, each vanadium nucleus is coupled through an oxygen bridge to four *nn* nickel ions in one chain and to two *nn* ions in the neighboring chain. As the vanadium-nickel distances and the bridging angles are very similar,²⁰ it is reasonable to first assume a common value of the isotropic hyperfine coupling, evaluated in Eq. (3). On the contrary, a reduced hyperfine coupling was considered for Co^{2+} impurities, $(A_{ij}^{\text{iso}})^i = A_{ij}^{\text{iso}} J_{i,h} = J$, in accordance with the reduction of the impurity-host exchange $J_{i,h}$ with respect to the *nn* intrachain exchange J .²² From the distributions of the average electron spin values sensed by ^{51}V nuclei, “stick” diagrams of the NMR spectra could be obtained. These diagrams were then convoluted by a homogeneously broadened Lorentzian line with the linewidth corresponding to the room-temperature experimental spectra.

1. Mg-doping

The temperature evolution of the simulated spectra for $\text{PbNi}_{1.88}\text{Mg}_{0.12}\text{V}_2\text{O}_8$ and $\text{PbNi}_{1.76}\text{Mg}_{0.24}\text{V}_2\text{O}_8$ is presented in Fig. 3(b) and Fig. 4(b), respectively. The solid lines are calculated on the assumption of temperature independent homogeneous broadening, which corresponds to the case of the parent compound, where the lineshape is given by the quadrupole Hamiltonian. Although the exact agreement with the experimental spectra at lower

temperatures is not reached, the impurity-induced shift of a significant portion of the signal towards higher frequencies is in a nice qualitative agreement with the asymmetric broadening of the NMR spectra observed in both Mg-doped samples. When a temperature dependent homogeneous broadening of the lines is assumed, the experimental NMR spectra are adequately reproduced, as shown by the dashed lines in Fig. 3(b) and Fig. 4(b). The fits were made down to 10 K because at lower temperatures the assumed Curie dependence should become inappropriate due to the proximity with the antiferromagnetic phase region. The predicted spectrum at 10 K is calculated with 3-times larger homogeneous broadening than the spectrum at room temperature. The necessity of including enhanced homogeneous broadening at temperatures significantly above the ordering temperature in low magnetic fields reopens our initial assumptions that the three-dimensional ordering effects resulting in the broadening of the NMR spectra, should be important already at rather high temperatures.²⁷

This model can be also used for the prediction of the NMR frequency shift. The calculated temperature-dependence is given in Fig. 7(a) by a dashed and a solid lines, for the cases of $\text{PbNi}_{1.88}\text{Mg}_{0.12}\text{V}_2\text{O}_8$ and $\text{PbNi}_{1.76}\text{Mg}_{0.24}\text{V}_2\text{O}_8$, respectively. At lower temperatures approximately 1.5-times larger shifts are predicted than measured. This can be understood as a consequence of the simplicity of our model taking into consideration the Curie dependence of the staggered moments. Such assumption is reasonable in the paramagnetic phase, yet close to the phase-transition point a pronounced reduction of the moments is expected. Moreover, also the correlation length should be affected by the vicinity of the magnetically ordered phase. The increased correlation length produces less inhomogeneous distribution of the spins sensed by the vanadium nuclei and thus lower NMR shifts.

2. Co-doping

The calculated spectra in the case of the $\text{PbNi}_{1.92}\text{Co}_{0.08}\text{V}_2\text{O}_8$ compound are presented in Fig. 5(b). At temperatures $T \gg T_{\text{N}}$ (14 K) a paramagnetic order of each impurity spin and both impurity-induced staggered spins is expected, which corresponds to the fits given by the solid lines. At the other temperature limit, $T \ll T_{\text{N}}$, antiferromagnetic correlations, producing effective spin $S = 1/2$ at impurity sites are anticipated. The simulated spectra with such correlations are presented by dashed lines and agree reasonably with the measurements. The simulations show slight broadening at lower temperatures because of the impurity-generated inhomogeneities in the electron spin distribution. However, experimental spectra suggest that also the homogeneous broadening must be enhanced below approximately 20 K, which can be understood as a precursor effect due to the proximity

with the antiferromagnetic phase transition.

The phase transition into the magnetically ordered state occurs at approximately 6 K in the magnetic field of 6.34 T. Below this temperature the NMR spectra exhibit strong broadening and the lineshape turns into a symmetric two-peak structure²⁸ as shown in Fig. 5(a). Such lineshape can be regarded as a signature of the bipartite spin lattice corresponding to the antiferromagnetic order. However, as vanadium nuclei sense averaged electron spin value over several sites, nonequivalent Ni-V bonds are required. Different values of the coupling are plausible since the Ni-V distances range from 3.33 Å to 3.48 Å and the Ni-O-V bridging angles are spanned from 123 to 135° in $\text{PbNi}_{1.88}\text{Mg}_{0.12}\text{V}_2\text{O}_8$,²⁰ which has a similar crystal structure to the $\text{PbNi}_{1.92}\text{Co}_{0.08}\text{V}_2\text{O}_8$ compound.

As seen from the simulated NMR spectra assuming antiferromagnetic ordering of each Co^{2+} impurity spin and the two staggered spins liberated next to it (Fig. 5), the observed low-temperature discrepancy between the ^{51}V NMR line position shown in Fig. 7(a) and the corresponding dc susceptibility of the $\text{PbNi}_{1.92}\text{Co}_{0.08}\text{V}_2\text{O}_8$ sample (Fig. 1) can be satisfactorily explained. It is due to the combined effect of the antiferromagnetic correlations and the reduced transferred hyperfine coupling of the vanadium nuclei with cobalt spins with respect to coupling to nickel spins. Even more, the predicted NMR shifts at low temperatures displace the lines slightly below the value of $\nu_{\text{L}} = 71.5$ MHz. Such negative shifts give a firm evidence for the validity of the presented model.

The simulated spectra assuming antiferromagnetic correlations between each impurity spin and the two liberated host spins also provide an adequate explanation why the inhomogeneous broadening of the NMR spectra in Co-doped samples is severely reduced with respect to the case of Mg-doping. The reason for the observed difference lies in the combined effect of the antiferromagnetic order and the reduced value of the cobalt-vanadium transferred hyperfine exchange. Next, there seems to exist a difference also in the intrinsic homogeneous broadening required to reproduce the low temperature spectra. Surprisingly, this parameter is larger in the case of the nonmagnetic doping, at least not in the extreme vicinity of the phase-transition temperature. This unexpected observation can be further inspected by analyzing the NMR spin-lattice relaxation, which similarly displays the temperature evolution of the electron spin correlations.

C. Diverse nature of the electron spin correlations as detected by the ^{51}V spin-lattice relaxation

The nuclear spin-lattice relaxation due to the hyperfine interaction, given by Eq. (2), is related to the transverse components of the electron spin fluctuation $\mathbf{S} = \langle \mathbf{S} \rangle$.^{29,30} In the case of the dominant isotropic hyperfine coupling the spin-lattice relaxation rate is determined by the transverse spin correlations $\hbar S_{\mathbf{q}}^+ (\omega) S_{\mathbf{q}} (0) i$, with \mathbf{q} being a wave vector. In the high-temperature approxi-

mation the spin-lattice relaxation is given by³⁶

$$\frac{1}{T_1 T} = \frac{k_B}{2\pi^2} \sum_{\mathbf{q}} A_{\mathbf{q}}^{\text{iso}} A_{\mathbf{q}}^{\text{iso}} \frac{\omega(\mathbf{q}; \mathbf{l}_L)}{\mathbf{l}_L}; \quad (5)$$

where $A_{\mathbf{q}}^{\text{iso}}$ is the Fourier transform of the isotropic hyperfine coupling and $\omega(\mathbf{q}; \mathbf{l}_L)$ represents the dissipative part of the transverse dynamical susceptibility.

When approaching the transition into the magnetically ordered state the spin-lattice relaxation is expected to exhibit critical dependence, due both to the divergent character of the static q -dependent susceptibility in the center of the antiferromagnetic zone, as well as due to the critical slowing down of the spin fluctuations.³⁰ It should be noted that the low-temperature increase of the spin-lattice relaxation is much more enhanced than the increase of the static uniform susceptibility reflected in the measurements of the dc susceptibility and the NMR shift, because the spin-lattice relaxation detects spin fluctuations at all wave vectors.

In Co-doped samples the above-mentioned expected behavior of the spin-lattice relaxation is shown in Fig. 6. The relaxation rate shows a strong temperature dependence close to the phase-transition temperature and the peak observed for $\text{PbNi}_{1.92}\text{Co}_{0.08}\text{V}_2\text{O}_8$ at 6 K nicely corresponds with the occurrence of the two-peak structure of the NMR spectra. On the contrary, the deviations of the spin-lattice relaxation in Mg-doped samples from the dependence observed in the pristine compound extend to much higher temperatures. At the same time, however, they are suppressed with respect to Co-doping at low temperatures. This observation suggests that the antiferromagnetic correlations are inhibited in Mg-doped samples by the magnetic field, which is in line with the bulk magnetization results in the magnetic field of 5 T (Fig. 1). Therefore, enhanced ferromagnetic correlations (reflected in increased $\omega(0; \mathbf{l}_L)$) should most likely be employed to account for both the spin-lattice relaxation behavior and the observed homogeneous broadening of the NMR spectra in the case of the nonmagnetic doping. The NMR broadening detects also longitudinal spin correlations in addition to the transversal correlations reflected in the spin-lattice relaxation.³⁰

D. Bulk magnetic properties

As experimentally verified by both the bulk magnetization and the NMR measurements, the magnetically ordered phase turns out to be much more robust against the magnetic field in the case of the magnetic Co-doping than in the case of the nonmagnetic Mg-doping. The metamagnetic transition occurring around 1.4 T in the $\text{PbNi}_{1.88}\text{Mg}_{0.12}\text{V}_2\text{O}_8$ at 2 K is a consequence of a strong easy-axis single-ion anisotropy D at each Ni^{2+} site,¹⁹ which is in accord with the inelastic neutron scattering measurements, suggesting $D = 5.2$ K.³⁷

In general, phase-diagrams of uniaxial Heisenberg antiferromagnets show three distinct phases depending on

the value of the single-ion anisotropy and the temperature; the paramagnetic phase, the antiferromagnetic phase and the spin-flop phase between them. In the mean-field approximation of the exchange interaction, it was theoretically predicted for $S = 1$ spin systems that a direct metamagnetic transition from the antiferromagnetic to the paramagnetic phase occurs in magnetic fields below $B_c = zJ_0/g_B$, if $D > zJ_0$ (z is the coordination number and J_0 is the exchange constant), with the critical field decreasing with temperature.³⁸ In the present case of the one-dimensional spin system, which is in addition highly inhomogeneous, the part of the exchange coupling constant zJ_0 is taken by the effective coupling providing the three-dimensional magnetic ordering. The single-ion anisotropy value $D = 5.2$ K should thus be compared to the phase-transition temperature $T_N = 3.4$ K. The zero-temperature value of the critical field is then expected to be of the order $B_c = k_B T_N / g_B = 2.7$ T. The magnetic field above the critical value breaks the three-dimensional magnetic correlations between staggered moments. However, due to the rather low value of the observed critical field, the antiferromagnetic spin correlations within the individual staggered moments should not be affected as they are governed by the strong nn intrachain exchange. Such behavior was very recently proposed to take place in lightly Mg-doped CuGeO_3 compounds, where a field-controlled microscopic separation of the antiferromagnetic and the paramagnetic phase was achieved.³⁹

On the other hand, the magnetic ordering in the Co-doped samples is preserved even in magnetic fields above 6 T as concluded from our NMR measurement. At low doping concentrations of either magnetic or nonmagnetic impurities the indirect staggered exchange¹² $J_s(\mathbf{L}) = (1/2)J \exp[-(\mathbf{L} - \mathbf{1})]$ mediated by the gapped Haldane medium, plays the dominant role in determining the stability of the magnetic order. This prediction is confirmed by the strong impurity-concentration dependence of the phase-transition temperatures at low doping levels in both cases.²⁴ However, at larger doping levels the cross-impurity exchange and the interchain exchange between staggered moments, as weaker exchange coupling mechanisms compared to the indirect staggered exchange, determine the stability of the magnetic order. The observation of the improved stability of the magnetically order phase in Co-doped samples can then be attributed to the significantly enhanced three-dimensional coupling of the impurity-induced staggered moments. The Co^{2+} impurities provide strong coupling between the two neighboring liberated spin $S = 1/2$ degrees of freedom due to the strong impurity-host exchange, as well as a firmer interchain connections. In addition, due to the strong spin-orbit coupling with respect to the crystal-field splitting for Co^{2+} ions,⁴⁰ an anisotropic exchange is generally observed for these ions. Such anisotropy, which reduces the spin fluctuations and thus enhances the stability of the magnetically ordered state, should prove highly important in the case of the

Co-doping. Namely, doping with Co^{2+} ions results in by far highest phase-transition temperatures with respect to other magnetic impurities.²⁴

Although, conceptionally, the impurity-induced long-range ordering in different spin-gap systems should have a common origin, the system dependent magnetic properties determining the stability of the ordered state must not be neglected in future theoretical studies. For instance, as extensive work on doping the spin-Peierls CuGeO_3 compound has shown, the spin of the dopants has only a minor influence on the phase-transition temperature and the spin-flop behavior of the antiferromagnetically ordered state. On the contrary, we have shown that the stability of the magnetically ordered state in the $\text{PbNi}_2\text{V}_2\text{O}_8$ Haldane compound crucially depends on the magnetic nature of the impurities.

V. CONCLUSIONS

We have presented a study of the impurity-induced magnetic ordering in the Haldane chain compound $\text{PbNi}_2\text{V}_2\text{O}_8$. An intrinsic difference between the effects of the nonmagnetic Mg^{2+} and the magnetic Co^{2+} impurities was observed. The long-range magnetic order was shown to be destroyed in Mg-doped samples at rather low magnetic fields implying that the antiferromagnetic correlations within the impurity-liberated staggered magnetic moments should stay preserved, as they are governed by the strong nn intrachain exchange. On the other hand, the ^{51}V NMR as well as the bulk magnetization measurements gave a clear indication of the improved stability of the antiferromagnetic order in the Co-doped samples. This experimental finding was attributed to the enhanced three-dimensional magnetic interactions between localized staggered moments, provided by the substantial anisotropic exchange coupling between impurity and host spins.

The staggered nature of the liberated degrees of freedom was indirectly explored through the appearance of

the ^{51}V NMR spectra. It was shown, that the broadening of the spectra as well as the line shift correspond to the Curie dependence of the impurity-induced staggered magnetic moments, delocalized on the scale of the theoretically predicted correlation length. An expected deviation of the model predictions from the experimental results was found only in the vicinity of the phase transition. In addition, the NMR measurements offered information about the different character of the electron spin correlations for both types of doping. In Co-doped samples the critical behavior of the NMR line broadening and the spin-lattice relaxation was detected at temperatures close to the phase transition. On the other hand, the pronounced homogeneous broadening of the NMR spectra and the enhanced spin-lattice relaxation was observed in Mg-doped samples at surprisingly high temperatures, despite the suppression of the antiferromagnetic correlations upon the magnetic field, as detected by the bulk magnetization measurements. This should be due to the enhanced spin correlations at $\mathbf{q} = 0$. It is envisaged that this surprising behavior of the spin correlations in the nonmagnetically doped samples can be further inspected by the complementary inelastic neutron scattering (INS) measurements. As this experimental technique provides both spectral and spacial information about spin fluctuations, it should uncover additional important aspects of the magnetic-field driven transformation, encompassing the nature of the spin fluctuations during the metamagnetic transition in the doped Haldane-chain $\text{PbNi}_2\text{V}_2\text{O}_8$ compound.

Acknowledgments

We acknowledge the financial support provided by the General Secretariat for Science & Technology (Greece) and the former Ministry of Education, Science and Sport of the Republic of Slovenia through a Greece-Slovenia “Joint Research & Technology Program”.

Electronic address: andrej.zorko@ijs.si

- ¹ S. H. Pan, E. W. Hudson, K. M. Lang, H. Eisaki, S. Uchida and J. C. Davis, *Nature*, **403**, 746, (2000).
- ² E. W. Hudson, K. M. Lang, V. Madhavan, S. H. Pan, H. Eisaki, S. Uchida and J. C. Davis, *Nature*, **411**, 920, (2001).
- ³ M. Hase, I. Terasaki, Y. Sasago, K. Uchinokura and H. Obara, *Phys. Rev. Lett.*, **71**, 4059, (1993).
- ⁴ M. Azuma, Y. Fujishiro, M. Takano, M. Nohara and H. Takagi, *Phys. Rev. B*, **55**, R8658, (1997).
- ⁵ M. Hagiwara, K. Katsumata, I. Affleck, B. I. Halperin and J. P. Renard, *Phys. Rev. Lett.*, **65**, 3181, (1990).
- ⁶ S. Eggert and I. Affleck, *Phys. Rev. Lett.*, **75**, 934, (1995).
- ⁷ N. Bulut, D. Hone, D. J. Scalapino and E. Y. Loh, *Phys. Rev. Lett.*, **62**, 2192, (1989).
- ⁸ G. B. Martins, M. Laukamp, J. Riera and E. Dagotto,

- Phys. Rev. Lett.*, **78**, 3563, (1997).
- ⁹ M. Laukamp, G. B. Martins, C. Gazza, A. L. Malvezzi, E. Dagotto, P. M. Hansen, A. C. Lopez, J. Riera, *Phys. Rev. B*, **57**, 10755, (1998).
- ¹⁰ Y. Motome, N. Katoh, N. Furukawa and M. Imada, *J. Phys. Soc. Jpn.*, **65**, 1949, (1996).
- ¹¹ S. Miyashita and S. Yamamoto, *Phys. Rev. B*, **48**, 913, (1993).
- ¹² E. S. Sørensen and I. Affleck, *Phys. Rev. B*, **49**, 15771, (1994).
- ¹³ F. Tedoldi, R. Santachiara and M. Horvatic, *Phys. Rev. Lett.*, **83**, 412, (1999).
- ¹⁴ J. Das, A. V. Mahajan, J. Bobroff, H. Alloul, F. Alet and E. S. Sørensen, *Phys. Rev. B*, **69**, 144404, (2004).
- ¹⁵ A. Oosawa, T. Ono and H. Tanaka, *Phys. Rev. B*, **66**, 020405(R), (2002).

- ¹⁶ Y. Uchiyama, Y. Sasago, I. Tsukada, K. Uchinokura, A. Zheludev, T. Hayashi, N. Miura and P. Böni, *Phys. Rev. Lett.*, **83**, 632, (1999).
- ¹⁷ R. Mélin, *Eur. Phys. J. B*, **18**, 263, (2000).
- ¹⁸ S. Inakagi and H. Fukuyama, *J. Phys. Soc. Jpn.*, **52**, 3620, (1983).
- ¹⁹ A. Lappas, V. Alexandrakis, J. Giapintzakis, V. Pomjakushin, K. Prassides and A. Schenck, *Phys. Rev. B*, **66**, 014428, (2002).
- ²⁰ I. Mastoraki, A. Lappas, J. Giapintzakis, D. Többens and J. Hernández-Velasco, *J. Solid State Chem.*, **177**, 2404, (2004).
- ²¹ I. Mastoraki, A. Lappas, R. Schneider and J. Giapintzakis, *Appl. Phys. A Suppl.*, **74**, S640, (2002).
- ²² A. Zorko, D. Arčon, A. Lappas and Z. Jaglicic, *arXiv:cond-mat/0506058* (2005, unpublished).
- ²³ K. Uchinokura, Y. Uchiyama, T. Masuda, Y. Sasago, I. Tsukada, A. Zheludev, T. Hayashi, N. Miura and P. Böni, *Physica B*, **284-288**, 1641, (2000).
- ²⁴ S. Imai, T. Masuda, T. Matsuoka and K. Uchinokura, *arXiv:cond-mat/0402595* (2004, unpublished).
- ²⁵ T. Masuda, K. Uchinokura, T. Hayashi and N. Miura, *Phys. Rev. B*, **66**, 174416, (2002).
- ²⁶ E. Stryjewski and N. Giorgano, *Adv. Phys.*, **26**, 487, (1977).
- ²⁷ D. Arčon, A. Zorko and A. Lappas, *Europhys. Lett.*, **65**, 109, (2004).
- ²⁸ A. Zorko, Ph.D. thesis, University of Ljubljana, 2004.
- ²⁹ T. Moriya, *Prog. Theor. Phys.*, **16**, 23, (1956).
- ³⁰ T. Moriya, *Prog. Theor. Phys.*, **28**, 371, (1962).
- ³¹ J. Sagi and I. Affleck, *Phys. Rev. B*, **53**, 9188, (1996).
- ³² V. Jaccarino, in *Magnetism, Vol IIA*, edited by G. T. Rado and H. Suhl (Academic Press, New York, 1965), p. 307.
- ³³ A. Zorko, D. Arčon, A. Lappas, J. Giapintzakis, C. Saylor and L. C. Brunel, *Phys. Rev. B*, **65**, 144449, (2002).
- ³⁴ Y. J. Kim, M. Greven, U. Wiese and R. J. Birgeneau, *Eur. Phys. J. B*, **4**, 291, (1998).
- ³⁵ F. Alet and E. S. Sørensen, *Phys. Rev. B*, **62**, 14116, (2000).
- ³⁶ T. Moriya, *J. Phys. Soc. Jpn.*, **18**, 516, (1963).
- ³⁷ A. Zheludev, T. Masuda, I. Tsukada, Y. Uchiyama, K. Uchinokura, P. Böni and S. H. Lee, *Phys. Rev. B*, **62**, 8921, (2000).
- ³⁸ I. Vilfan and B. Zeks, *J. Phys. C: Solid state Phys.*, **12**, 4295, (1979).
- ³⁹ V. N. Glazkov, A. I. Smirnov, H. A. Krug von Nidda, A. Loidl, K. Uchinokura and T. Masuda, *Phys. Rev. Lett.*, **94**, 057205, (2005).
- ⁴⁰ J. R. Pilbrow, *Transition Ion Electron Paramagnetic Resonance* (Oxford University Press, Oxford, 1990).